

Properties of Long Gamma-Ray Burst Host Galaxies in Cosmological Simulations

M.A. Campisi^{1*}, G. De Lucia^{1†}, L.-X. Li¹, S. Mao² and X. Kang³

¹ *Max-Planck-Institut für Astrophysik, Karl-Schwarzschild-Str. 1, D-85748 Garching, Germany*

² *Jodrell Bank Centre for Astrophysics, Alan Turing Building, University of Manchester, Manchester, M13 9PL, UK*

³ *Max-Planck-Institut für Astronomie, Königstuhl 17, 69117 Heidelberg, Germany*

Accepted ???. Received ???; in original form ???

ABSTRACT

We use galaxy catalogues constructed by combining high-resolution N-body simulations with semi-analytic models of galaxy formation to study the properties of Long Gamma-Ray Burst (LGRB) host galaxies. We assume that LGRBs originate from the death of massive young stars and analyse how results are affected by different metallicity constraints on the progenitor stars. As expected, the host sample with no metallicity restriction on the progenitor stars provides a perfect tracer of the cosmic star formation history. When LGRBs are required to be generated by low-metallicity stars, they trace a decreasing fraction of the cosmic star formation rate at lower redshift, as a consequence of the global increase in metallicity. We study the properties of host galaxies up to high redshift (~ 9), finding that they typically have low-metallicity ($Z < 0.5Z_{\odot}$) and that they are small ($M < 10^9 M_{\odot}$), bluer and younger than the average galaxy population, in agreement with observational data. They are also less clustered than typical L_* galaxies in the Universe, and their descendants are massive, red and reside in groups of galaxies with halo mass between $10^{13} M_{\odot}$ to $10^{14} M_{\odot}$.

Key words: gamma-rays: bursts – host galaxies .

1 INTRODUCTION

Gamma-ray bursts (GRBs) are the most energetic explosions in the Universe (Zhang & Mészáros 2004). As such, they offer exciting possibilities to study astrophysics in extreme conditions, e.g., radiative processes in highly relativistic ejecta (Huang et al. 2000; Fan & Piran 2008, and references therein). Because of their very large luminosity, GRBs represent “cosmological” events, which have been detected up to $z \sim 8.2$ (Tanvir et al. 2009; Salvaterra et al. 2009). It has been proposed that some tight correlations among GRB parameters can make them “standard candles” for probing the Universe to the high-redshift regime that supernovae Ia cannot attain (e.g. Ghirlanda et al. 2004; Dai et al. 2004; Zhang 2007, and references therein. See however Li 2007a,b, 2008a).

It is well-known that the duration distribution of GRBs is bimodal (Kouveliotou et al. 1993), dividing GRBs into two classes: long GRBs (hereafter LGRBs) and short GRBs, depending on whether their durations are longer or shorter than a few seconds. The observed properties of host galaxies of short and long GRBs indicate that they have different progenitors. LGRBs are

typically found in star-forming galaxies, predominantly irregular dwarf galaxies (Conselice et al. 2005; Fruchter et al. 2006; Wainwright et al. 2007). In contrast, short GRBs are found in both early-type and late-type galaxies. Many models have been proposed for explaining the origin of these two classes of GRBs. The currently favourite hypotheses are that short GRBs are produced by the merger of compact objects – between two neutron stars or between a neutron star and a black hole (Li & Paczyński 1998; O’Shaughnessy et al. 2008), while LGRBs originate from the death of massive stars (with low metallicity), such as Wolf-Rayet stars. This scenario for the formation of LGRBs is usually referred to as the “collapsar model” (Yoon et al. 2006, 2008; Woosley & Heger 2006).

Observational data are consistent with the hypothesis of a LGRB-supernova connection: at least some LGRBs are associated with core-collapse supernovae (Galama et al. 1998; Li 2006; Woosley & Heger 2006, and references therein). In addition, all supernovae associated with GRBs are Type Ic, which supports the hypothesis of Wolf-Rayet stars as progenitors of LGRBs. Because of their connection with supernovae, LGRBs are potential tracers of the cosmic star formation history (Totani 1997; Wijers et al. 1998; Mao & Mo 1998; Porciani & Madau 2001). To date, there are 130 GRBs with known redshift and 50 with estimated host galaxy stellar mass (Savaglio et al. 2008). Given the difficulty in detecting and localizing short GRBs, most of the observational studies about host

* E-mail: campisi@mpa-garching.mpg.de

† INAF - Astronomical Observatory of Trieste, via G.B. Tiepoli 11, I-34131 Trieste, Italy.

	WMAP1	WMAP3
Ω_m	0.25	0.226
Ω_Λ	0.75	0.774
Ω_b	0.045	0.04
σ_8	0.9	0.722
h	0.73	0.743
n	1	0.947

Table 1. Cosmological parameters of the two simulations used in Wang et al. (2008). Ω_m , Ω_Λ , Ω_b represent the density of matter, dark energy, and baryons respectively. σ_8 and n are the amplitude of the mass density fluctuations, and the slope of the initial power spectrum. The Hubble constant is parameterised as $H_0 = 100 h \text{ km s}^{-1} \text{ Mpc}^{-1}$.

galaxies are for LGRBs, which will be the focus of this work. Studies of the physical properties of GRBs are not easy as they require deep targeted observations at high redshift. In addition, the probability for a chance superposition of GRBs and galaxies on the sky is significant for high- z GRBs, and $\sim 3\%$ for galaxies at $z < 1.5$ (Campisi & Li 2008).

The observational information gathered so far indicates that most LGRBs are found in faint star forming galaxies dominated by young stellar populations with a sub-solar gas-phase metallicities, although there are a few host galaxies with higher metal content (Prochaska et al. 2004; Wolf & Podsiadlowski 2007; Fynbo et al. 2006; Price et al. 2007; Savaglio et al. 2003; Savaglio 2006; Savaglio et al. 2008; Stanek et al. 2006, and references therein).

In this work, we analyse the properties of host galaxies of LGRBs, using a galaxy catalogue constructed by combining high-resolution N-body simulations with a semi-analytic model of galaxy formation. In particular, we use the models discussed in Wang et al. (2008) for two cosmological models with parameters taken from the first-year and the third-year Wilkinson Microwave Anisotropy Probe (WMAP) (Spergel et al. 2003) measurements. To select candidate host galaxies of LGRBs, we extract from the available semi-analytic galaxy catalogues the information for the age and metallicity of newly formed stars and we adopt the collapsar model. We built three samples of host galaxies with different metallicity thresholds, and we compare the properties of the selected galaxies with observational data, in particular the data in Savaglio et al. (2008). Compared with previous theoretical studies, the simulations used in our study have the largest volume, and they also allow us to explore the cosmological dependence. Finally, the information available from the semi-analytic catalogues enable us to study the clustering and descendant properties of LGRB hosts.

The paper is organised as follows. We present in section 2 the simulated galaxy catalogues used in this work. In section 3, we describe the method for selecting long GRB host galaxies. We describe our results in section 4. We discuss our results and give our conclusions in section 5.

2 THE SIMULATED GALAXY CATALOGUES

In this study, we use the galaxy catalogues constructed by Wang et al. (2008) for two simulations with cosmological parameters from the first and third-year WMAP results. The two sets of cosmological parameters are listed in Table 1. As discussed in Wang et al. (2008), the most significant differences between WMAP1 and WMAP3 cosmological parameters are a lower value

of σ_8 and a redder (smaller) primordial power spectrum index n in WMAP3, resulting in a significant delay for structure formation. Both simulations correspond to a box of $125 h^{-1} \text{ Mpc}$ comoving length and a particle mass 8.6×10^8 (WMAP1) and $7.8 \times 10^8 M_\odot$ (WMAP3). The softening length is $5 h^{-1} \text{ kpc}$ in both simulations (see Table 2 in Wang et al. 2008). Simulation data were stored in 64 outputs, that are approximately logarithmically spaced in time between $z = 20$ and $z = 1$, and linearly spaced in time for $z < 1$. Each simulation output was analysed with the post-processing software originally developed for the Millennium Simulation (Springel et al. 2005).

Merging history trees for self-bound structures extracted from the simulations were used as input for the Munich semi-analytic model of galaxy formation. Interested readers are referred to Croton et al. (2006), De Lucia & Blaizot (2007) and references therein for details on the physical processes explicitly modelled. Previous work has shown that the galaxy population predicted by this particular model provides a reasonably good match with the observed local galaxies properties and relations among stellar mass, gas mass, and metallicity (De Lucia, Kauffmann & White 2004), luminosity, colour, morphology distributions (Croton et al. 2006; De Lucia et al. 2006), and the observed two-point correlation functions (Springel et al. 2005; Wang et al. 2008). In addition, Kitzbichler & White (2007) have shown that the model also agrees reasonably well with the observed galaxy luminosity and mass function at higher redshift.

We remind the reader that the models discussed in Wang et al. (2008) adopt the same physics, but different combinations of model parameters are used for the simulations with WMAP1 and WMAP3 cosmology. The WMAP1 simulation uses the same parameters (and physical model) adopted in De Lucia & Blaizot (2007). For the WMAP3 simulation, the model adopts lower supernovae and AGN feedback efficiencies in order to compensate for the delay in structure formation obtained with a lower σ_8 . This combination of model parameters corresponds to the WMAP3B model used in Wang et al. (2008). The alternative model WMAP3C used in that paper leads to very similar results and so will not be discussed further in this paper. In the following, we limit our analysis to galaxies with stellar mass larger than $2 \times 10^8 M_\odot$, which is above the resolution limit of the N-body simulations used.

We note that the most recent cosmological model from the five-year data of WMAP is between WMAP1 and WMAP3, so the results from the two simulations used here are expected to bracket results from a simulation with the 5-year WMAP cosmology.

3 IDENTIFICATION OF LGRB HOST GALAXIES

In order to identify candidate GRB host galaxies, we adopt the collapsar model for LGRBs: all young stars with mass $> 30 M_\odot$ ending their life with a supernova should be able to create a BH remnant. If the collapsar has high angular momentum, the formation of the BH is accompanied by a GRB event (Yoon et al. 2006, 2008). As mentioned in Sec. 1, recent studies on the final evolutionary stages of massive stars have suggested that a Wolf-Rayet (WR) star can produce a LGRB if its mass loss rate is small, which is possible only if the metallicity of the star is very low. When metallicities are lower than $\sim 0.1 - 0.3 Z_\odot$, the specific angular momentum of the progenitor allows the loss of the hydrogen envelope while preserving the helium core (Woosley & Heger 2006; Fryer, Woosley & Hartmann 1999). The loss of the envelope reduces the material that the jet needs to cross in order to escape,

	$N[M_{\odot}^{-1}]$	$m_{*,\min}$	$m_{*,\max}$
SNe	7.421×10^{-3}	8	100
BH	1.035×10^{-3}	30	100

Table 2. Number of SNe and BHs per solar mass of stars formed, using a Salpeter IMF.

while the helium core should be massive enough to collapse and power a GRB.

In order to construct our host galaxy sample, we have extracted from the available semi-analytic catalogues the information about the age and metallicity of all stars. We have then created the following host samples:

- (i) HOST1, obtained by selecting galaxies containing stars with age $< t_c = 5 \times 10^7$ yr;
- (ii) HOST2, including galaxies with stars of age $< t_c$ and metallicity $Z \leq 0.3 Z_{\odot}$;
- (iii) HOST3, defined by selecting galaxies containing stars with age $< t_c$ and metallicity $Z \leq 0.1 Z_{\odot}$.

In order to count the number of GRB events in each galaxy, we make use of two important pieces of information: (a) the rate of GRB with respect to the SNe explosions (without any cut in metallicity for the progenitors stars); (b) the rate of very massive stars (producing remnant BHs) as a function of redshift and metallicity with respect to the total number of SNe events. In this way we are able to count how many BHs with low metallicity progenitors will produce GRBs.

We assume a Salpeter Initial Mass Function (IMF) and compute the number of stars ending their lives as supernovae (SNe) or as black-holes (BHs) per unit mass of stars formed by:

$$N = \frac{\int_{m_{*,\min}}^{m_{*,\max}} \phi(m_*) dm_*}{\int_{0.1}^{m_{*,\max}} m_* \phi(m_*) dm_*}, \quad (1)$$

where $\phi(m_*)$ is the IMF, $m_{*,\min}$ is the minimum initial mass to form a supernova or a black hole, and $m_{*,\max}$ is the upper limit of the mass function. We take $m_{*,\min}$ to be $8 M_{\odot}$ for SNe and $30 M_{\odot}$ for BHs (Fryer et al. 1999), and $m_{*,\max} = 100 M_{\odot}$ (the lower limit of the IMF is taken to be $0.1 M_{\odot}$). Eq. 1, evaluated for progenitor stars of all metallicities, provides the numbers listed in Table 2.

Without any restriction on the metallicity of the progenitor stars, the relative number of BHs and supernovae is ~ 14 per cent (140 BHs per 1000 SNe). When considering the metallicity threshold for BHs, the rate is reduced and varies with redshift (Langer & Norman 2006; Wolf & Podsiadlowski 2007). This is illustrated in Fig. 1 for the two different metallicity thresholds adopted in our study. At low redshift, there are from 0.1 to 6 low-metallicity BHs formed per 1000 SNe. The rate grows with increasing redshift, reaching values between ~ 10 ($Z < 0.1 Z_{\odot}$) and ~ 70 ($Z < 0.3 Z_{\odot}$) at redshift ~ 9 .

Integrating over the redshift, Fig. 1 allows us to calculate the average ratio between the number of black holes from different progenitors and the number of supernovae in the Universe. However, not every black hole will produce a LGRB. To normalise the LGRB abundance, we assume that the rate of GRB per SNe is on average (over all cosmic times) of about 1 GRB event every 1000

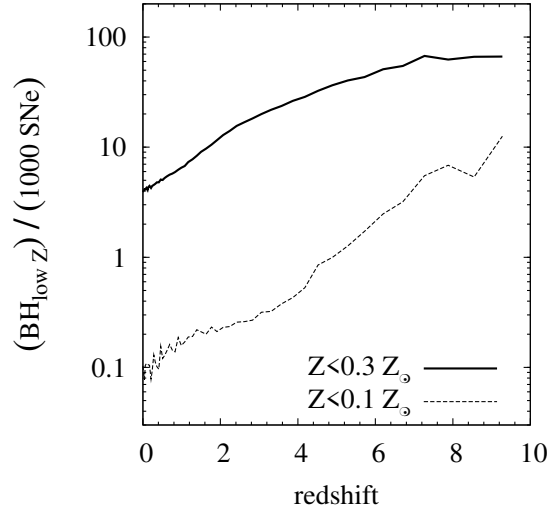


Figure 1. Number of low-Z BHs per 1000 SNe as a function of redshift, for progenitor stars with metallicity lower than $0.3 Z_{\odot}$ and $0.1 Z_{\odot}$. Results are shown for the model WMAP3B. Similar results are obtained in the WMAP1 case.

SNe (Porciani & Madau 2001; Langer & Norman 2006). The number of LGRBs relative to the black holes in the three samples (with or without the metallicity cutoff) is given by

$$R_{\text{GRB}} = \frac{\text{GRBs}}{\text{BH}_{\text{lowZ}}} = \frac{\text{GRBs}}{1000\text{SNe}} \times \left\langle \frac{1000\text{SNe}}{\text{BH}_{\text{lowZ}}} \right\rangle. \quad (2)$$

where the last term is obtained by integrating over redshift (or cosmic time). For the HOST1 sample, the last term is a constant ($1/140$), and thus $R_{\text{GRB}} \sim 0.007$; for the other two samples, we obtain $R_{\text{GRB}} \sim 0.056$ and ~ 1 .

For each galaxy in the simulation box, we can count how many BHs are produced from low metallicity progenitors and then obtain the corresponding number of LGRBs:

$$N_{\text{LGRBs}} = \text{BH}_{\text{lowZ}} \times R_{\text{GRB}}.$$

It is important to note that our model provides only an upper limit to the number of LGRB events because the formation of BHs and low metallicity are only two of many requirements for the production of LGRBs. E.g., high spin of the progenitor star is another requirement that cannot be handled in our model. In the following, we consider each galaxy hosting at least one GRB event ($N_{\text{LGRBs}} \geq 1$) as a ‘host galaxy’.

There are relatively few galaxies with $N_{\text{LGRBs}} < 1$ and their inclusion does not change our results significantly.

We stress that we are not using the (average) galaxy metallicity to select our host galaxy samples, but the metallicity of each ‘pocket’ of stars formed at each time-step. Stars are assumed to form with the metallicity of the interstellar medium at the time of star formation, and the model adopts an instantaneous recycling approximation for metal enrichment. So, the gas-phase metallicity of host galaxies will generally be higher than the metallicity threshold we have adopted for our samples.

Note that the LGRB rate computed above is not directly comparable to the observed rate because that would require us to take into account many unknown factors like the jet angle, and to include any possible observational bias (see Lapi et al. 2008; Li 2008b).

4 RESULTS

In this section, we discuss the physical properties of LGRB hosts selected using the procedure described in Sec. 3. In particular, we compare the LGRB rate to the cosmic star formation rate (Sec. 4.1), and the properties of LGRBs hosts to the global properties of galaxies at the same cosmic epoch (Sec. 4.2). When we study the average or median property of the host galaxies we weigh each host by the likelihood that it contains a GRB. That allow us to compare with observed data since the galaxies which host many GRBs are proportionally more likely to appear in any given observed sample. We also study the typical environment (Sec. 4.3) and evolutionary stage (Sec. 4.4) of LGRB host galaxies.

4.1 The cosmic star formation rate versus the LGRB rate

The collapsar model links LGRBs to the evolution of single massive stars whose lifetimes are negligible on cosmological scales. If no other condition is required for producing a LGRB event, then the rate of LGRBs should be an unbiased tracer of the global star formation in the Universe (e.g. Totani 1997; Wijers et al. 1998; Mao & Mo 1998; Porciani & Madau 2001; Bromm & Loeb 2002; Fynbo et al. 2006; Price et al. 2006; Savaglio 2006; Totani et al. 2006; Prochaska et al. 2007; Li 2008b, and references therein). Fynbo et al. (2008) have recently suggested that GRB and Damped Lyman-Alpha samples, in contrast with magnitude limited samples, provide an almost complete census of $z \sim 3$ star-forming galaxies. We note, however, that the sample used in this study are biased against high-metallicity and dusty systems.

However, both observations and theoretical studies indicate that the metallicity of the progenitor star plays an important role in setting the necessary conditions for a LGRB explosion. In this case, the rate of LGRBs is expected to be a biased tracer of the cosmic star formation rate. This is demonstrated explicitly in Fig. 2, which compares the cosmic star formation rate obtained using all galaxies in the simulation box to that obtained for the three LGRB host samples defined in the Sec. 3.

The sample with no threshold on metallicity (HOST1) traces exactly the global star formation rate (solid line in Fig. 2). This is not the case for the two samples with metallicity thresholds (HOST2 - dot-dashed line and HOST3 - dashed line). For the HOST2 and HOST3 samples, the LGRB rate peaks at higher redshift than the cosmic star formation rate, as a consequence of the global decrease of metallicity with increasing redshift. At higher redshift, the mean metallicity of the intergalactic medium is lower, which implies that a larger fraction of stars form below the metallicity thresholds adopted for HOST2 and HOST3. Therefore the deviation of the LGRB rate from the star formation rate decreases with increasing redshift. At $z \sim 9$, the HOST2 sample measures about 99 per cent of the global star formation density. The fraction decreases to about 30 per cent at $z \sim 5$ and to only about 10 per cent at present. For the HOST3 sample, the bias is even stronger because of the lower metallicity threshold: it traces only 30 per cent of the global star formation density at $z \sim 9$, and less than 10 per cent at $z < 5$. The results shown in Fig. 2 are in qualitative agreement with recent observational estimates (Kistler et al. 2008), and with recent theoretical studies also based on the collapsar model (Yoon, Langer & Norman 2006; Cen & Fang 2007; Nuza et al. 2007; Lapi et al. 2008).

Finally, Fig. 2 also shows that adopting a cosmological model compatible with third-year WMAP measurements (right panel), a delay is produced in the cosmic star formation rate, due to the delay

in structure formation. Except for this delay, the predicted trends are the same for the WMAP1 and WMAP3 simulations. In the following, we will only show results obtained using the WMAP3 simulation as those obtained for the WMAP1 simulation are very similar. In addition, we will focus only on the two host samples with metallicity thresholds (HOST2 and HOST3).

We remind the reader that we consider as ‘hosts’ all galaxies which can host at least one LGRB event between two simulation output. Since galaxies at higher redshift have lower metallicities and form stars at higher rates, the rate of LGRBs per host galaxy increases rapidly with redshift. The left panel in Fig. 3 shows the redshift evolution of the number of LGRBs (solid line) and of host galaxies (HOST3 - dashed line). The two vertical lines indicate the peaks of the distributions: the number of LGRBs peaks at $z \sim 5$, while the number of host galaxies is maximum at $z \sim 2$. The right panel of Fig. 3 shows the rate of LGRBs per galaxy and per Myr computed for the WMAP3 simulation and for the HOST3 sample. The predicted rate of LGRBs decreases from ~ 1000 at $z \sim 9$ to about $10 \text{ Myr}^{-1} \text{ galaxy}^{-1}$ at $z \sim 0$, in agreement with calculations by Fryer et al. (1999). Note that the LGRB rate computed above is not directly comparable to the observed rate because that would require us to take into account many unknown factors like the jet angle, and to include any possible observational bias (see Lapi et al. 2008; Li 2008b).

4.2 Physical properties of LGRB host galaxies

A number of recent papers have studied the physical properties of LGRB host galaxies using deep observations covering a large wavelength range, both in imaging and in spectroscopy. These studies have revealed that LGRB host galaxies are typically faint and star forming galaxies, dominated by young and metal-poor stellar populations (Le Floch et al. 2003; Fruchter et al. 2006; Wainwright et al. 2007; Savaglio et al. 2008). In this section, we analyse the physical properties of our model host galaxies, and compare these with the properties of the average galaxy population, and with observational estimates.

Fig. 4 shows the K-band rest-frame luminosity function of host galaxies for the HOST2 (dot-dashed line) and the HOST3 (dashed line) samples, compared with the galaxy luminosity function measured considering all galaxies in the simulation box, at different redshift. At all redshifts, LGRB host galaxies have luminosities well below the characteristic luminosity L_* , in agreement with observational measurements. While the total luminosity function evolves strongly with the redshift (particularly beyond $z \sim 1$), the number densities and the range of luminosities of LGRB host galaxies vary more mildly, due to the fact that at higher redshift a larger fraction of the whole galaxy population can host LGRBs.

Recent observational studies have focused on the stellar mass distribution of GRB host galaxies. Castro Cerón et al. (2008) have found that the typical stellar mass of host galaxies is smaller than the stellar mass of field galaxies at the same redshift. For a sample of 30 LGRB hosts, they provide estimates of the stellar mass between 10^7 and $10^{11} M_\odot$, with a mean value of $M_* \sim 10^{9.7} M_\odot$. About 70 per cent of the host galaxies in their sample have stellar mass $M_* < 10^{10.1} M_\odot$. Similar results have been found by Savaglio et al. (2008). Using a sample of 46 GRB hosts - the largest sample so far - they estimate a median stellar mass of $10^{9.3} M_\odot$, and find that about 83 per cent of the studied systems have stellar mass between $10^{8.5}$ and $10^{10.3} M_\odot$.

In Fig. 5 we compare the galaxy mass distribution for model host galaxies from the HOST2 and HOST3 samples to the distribu-

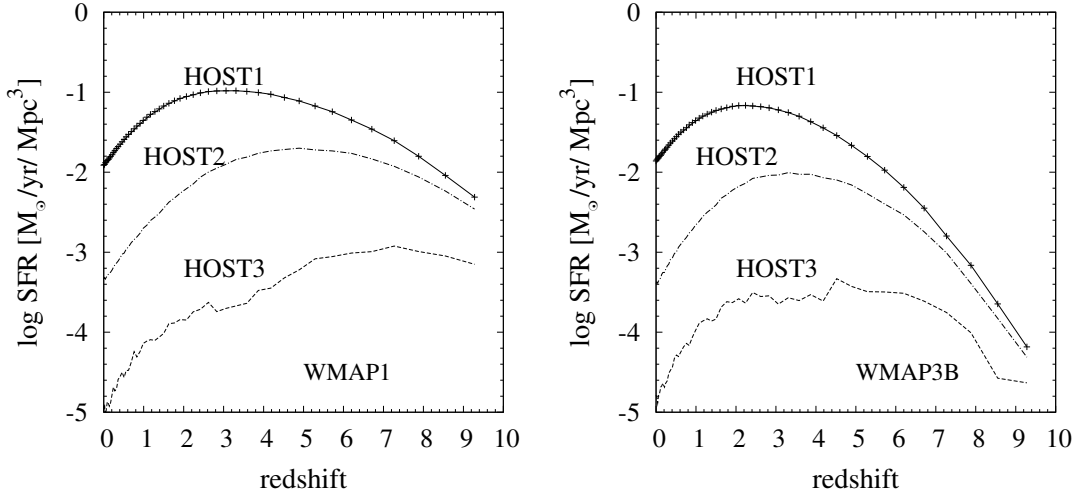


Figure 2. Log $SFR [M_{\odot} \text{ yr}^{-1} \text{ Mpc}^{-3}]$ as a function of redshift, computed for all galaxies in the simulation box (solid line). Left and right panels correspond to the WMAP1 and WMAP3 simulations respectively. The dot-dashed and dashed lines corresponds to the HOST2 and HOST3 samples. The sample with no threshold on metallicity (HOST1) traces exactly the global star formation rate measured considering all galaxies in the simulated boxes (solid line).

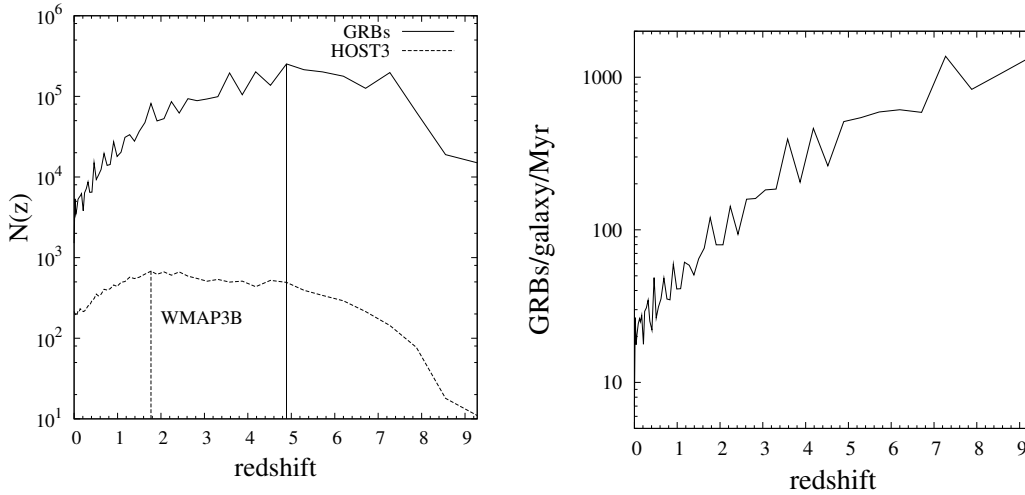


Figure 3. Left panel: redshift distribution of LGRB events (solid line) and of host galaxies (dashed line), for the sample HOST3 (with metallicity threshold $0.1 Z_{\odot}$). The vertical lines indicate the peaks of the distributions. Right panel: the rate of LGRBs per galaxy per Myr. Both panels correspond to results from the WMAP3 simulation.

tion obtained considering all galaxies in the simulated box. For this figure, all galaxies and hosts at all redshifts up to $z \sim 9$ have been used. Fig. 5 shows that LGRB host galaxies have typically low mass with a small fraction of them having stellar mass up to $\sim 10^{11} M_{\odot}$. About 90 per cent of the host galaxies have stellar mass $< 10^9 M_{\odot}$ and $< 10^{10} M_{\odot}$ for HOST3 and HOST2 respectively.

It is well known that the galaxy stellar mass is tightly correlated with the rest-frame K-band luminosity. Savaglio et al. (2008) have shown that this relation applies to GRB host galaxies as well, but they argue that GRB galaxies have on average higher luminosity than “field” galaxies with the same stellar mass, implying a lower M_*/L_K ratio, as expected for younger galaxies. We compare results from our model to observational measurements in Fig. 6. The dashed black line is the best-fit to the observational data by Savaglio et al. (2008): $\log M_* = -0.463 \times M_K - 0.102$. The red line in Fig. 6 shows the mean luminosity-mass relation obtained by using all galaxies in the simulation boxes up to $z \sim 9$. The

pink line shows the mean value for host galaxies in the HOST2 sample, and the blue line corresponds to the mean value obtained for the HOST3 sample. To compute the average of M_K we weigh each host by the likelihood that it contains a GRB. For this sample, we also show the quartiles of the distribution. We note that Savaglio et al. (2008) adopt a Baldry & Glazebrook IMF for their stellar mass estimates, while the model used in this study adopts a Chabrier IMF to compute model magnitudes. In order to compare model results with observational estimates, we have decreased the observed stellar mass by a factor 1.3. Fig. 6 shows that the K-band absolute magnitude distribution of simulated GRB host galaxies is in good agreement with observations. It also shows that, on average, host galaxies have stellar masses which are lower, although with a large scatter, than “typical” galaxies with the same mass, in agreement with observational findings.

In Fig. 7, we compare the median colour of model LGRB host galaxies with observational measurements by Savaglio et al. (2008,

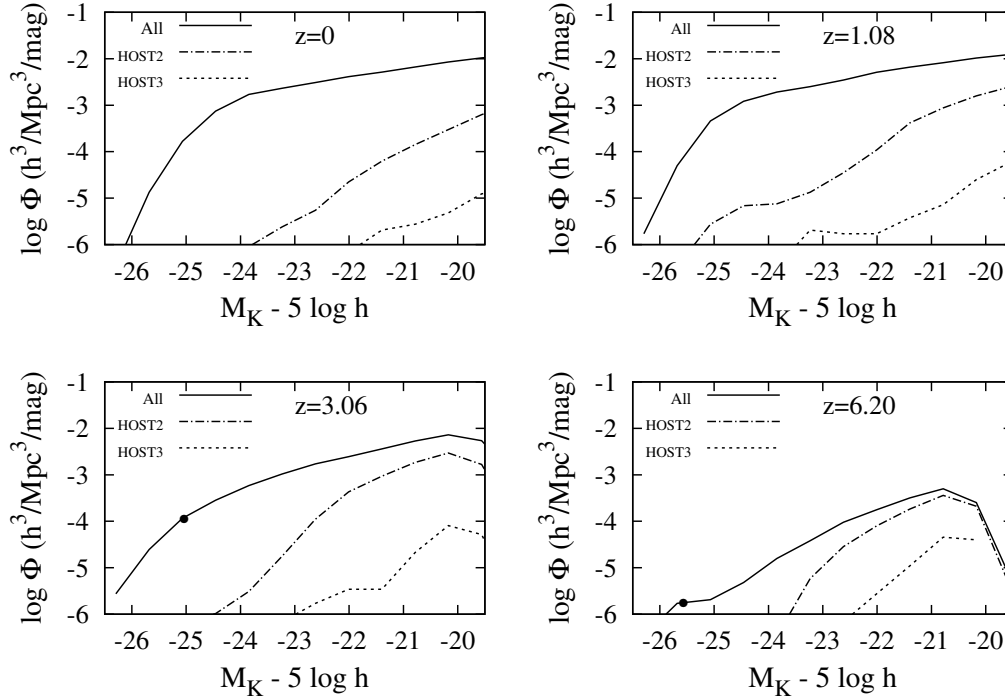


Figure 4. Luminosity function of the HOST2 (dot-dashed line) and the HOST3 (dashed line) samples, compared to the galaxy luminosity function measured using all galaxies in the simulation box (solid line). Different panels are for different redshifts: 0 (top left panel), 1.08 (top right panel), 3.06 (bottom left panel), and 6.20 (bottom right panel). In the last two panel the dark bullet shows the characteristic luminosity L_* .

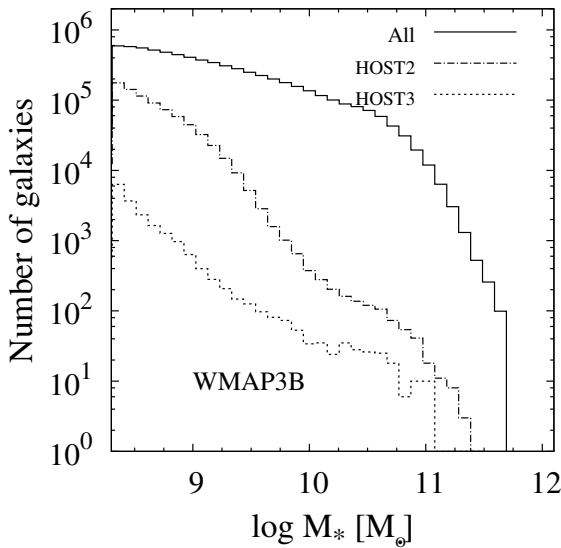


Figure 5. Galaxy mass function for the HOST2 (dot-dashed line) and HOST3 (dashed line) samples, compared to the galaxy mass function measured using all galaxies in the simulation box (solid line). All galaxies with $z \leq 9$ have been used in this figure.

shown as black symbols). Model results indicate that GRB galaxies are typically bluer than the average galaxy population at the same redshift. We note that the observed colours exhibit a quite large scatter, probably due to the unknown dust extinction.

Fig. 8 shows the median gas metallicity evolution for the

HOST3 sample (black crosses) compared with the observational estimates for the GRB-DLAs studied in Savaglio et al. (2006, 2008 - blue triangles with error bars a few show the lower and upper-branch metallicity solution in Savaglio et al. 2008). In order to compare with observations we weigh each host with the total number of LGRBs. The red line in Fig. 8 shows the median metallicity obtained using all galaxies in the simulation box. The figure shows that the metallicity of model galaxies (both “normal” and hosts) does not evolve significantly with redshift. The observational measurements exhibit a large scatter and have typically large uncertainties. Within these, model predictions are in relatively good agreement with observational data. It should be noted that the lack of evolution in the gas-phase metallicity of the HOST3 sample is essentially due to our selection method. In order to enter this sample, host galaxies must have young stars with metallicity lower than $Z \leq 0.1Z_{\odot}$. In the model used in this study, stars form with the metallicity of the gas-phase component, so the adopted selection requires host galaxies to have gas-phase metallicity close to the adopted threshold (it will be typically higher because the model adopts an instantaneous recycling approximation).

Another important and well studied relation is the luminosity-metallicity relation. This has been measured for a very large sample of star forming galaxies from the Sloan Digital Sky Survey (SDSS) by Tremonti et al. (2004), and for smaller samples of galaxies by other authors. In particular, Brown, Kewley & Geller (2008) have recently suggested a technique to identify extremely metal-poor galaxies which share very similar properties (age, metallicity, star formation rates) with hosts of LGRBs. The data from Brown et al. (2008) are plotted in Fig. 9 as blue circles, together with the observed relations by Tremonti et al. (2004), and by Richer & McCall (1995) for a sample of irregular galaxies. Model results for the

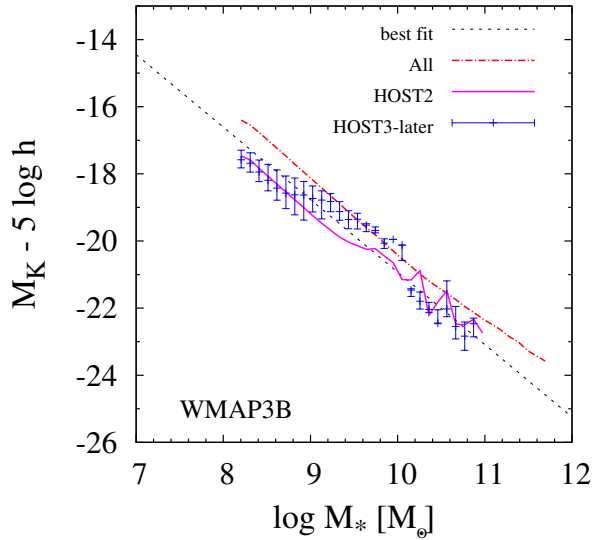


Figure 6. Mean K-band absolute magnitude as a function of stellar mass for all galaxies in the simulation (red line), for galaxies in the HOST2 sample (green), and for galaxies in the HOST3 sample (blue). For the HOST2 and HOST3 samples we compute the average of M_K weighing each host with the total number of LGRBs. Black symbols correspond to observational data from Savaglio et al. (2008), and the dotted black line is the fit provided by the same author ($\log M_* = -0.463 \times M_K - 0.102$).

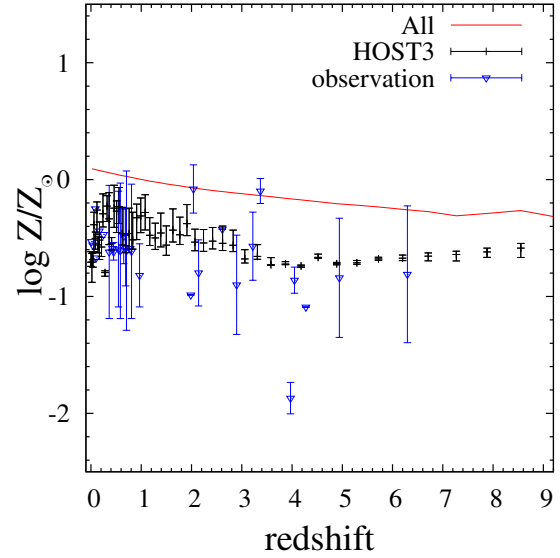


Figure 8. Median gas metallicity as a function of redshift for all galaxies in the simulation box (red line), and for galaxies from the HOST3 sample (dark crosses, error bars show the quartiles of the distributions). For HOST3 sample we compute the median gas metallicity weighing each host with the total number of LGRBs. The blue triangles are observational measurements for GRB-DLAs host galaxies from Savaglio (2006) and for the GRB host galaxies studied in Savaglio et al. (2008).

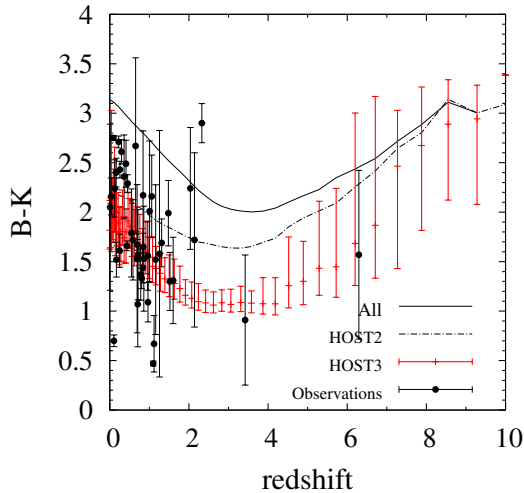


Figure 7. Median B-K colour as a function of redshift for observed GRB hosts (black crosses), all galaxies in the simulation (solid line), galaxies from the HOST2 sample (dot-dashed line), and galaxies from the HOST3 sample (red crosses). For the HOST2 and HOST3 samples we compute the median weighing each host with the total number of LGRBs.

HOST3 sample are plotted as magenta asterisks and lie in the same region occupied by the Brown et al. data. Dark crosses show the corresponding results for the HOST2 sample. As explained above, the adopted selection results in clear metallicity cuts in Fig. 9. Observational studies of gas-phase metallicity of GRB hosts could therefore provide important information on the metallicity of the progenitor stars, although inhomogeneous mixing of metals could complicate the interpretation. The few objects in the HOST3 sam-

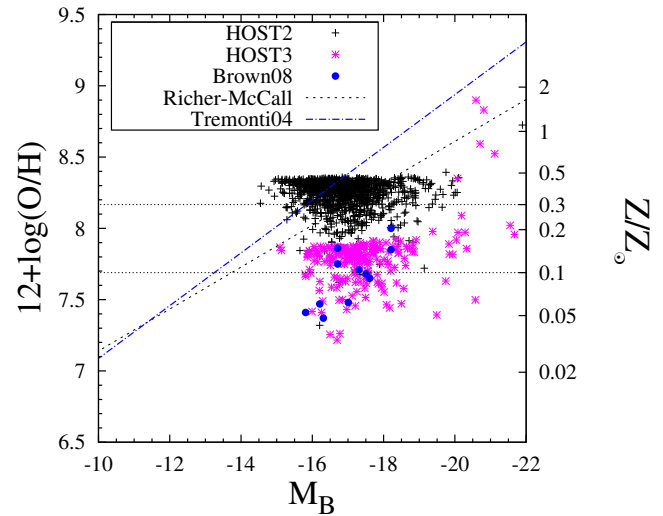


Figure 9. Gas metallicity as function of the B-band luminosity for model galaxies with $z < 0.1$ from the HOST3 (magenta asterisks) and HOST2 (black crosses) samples, compared with observational measurements by Brown et al. (2008, blue circles) for a sample of metal-poor galaxies. The blue-dashed and black-dotted lines show the metallicity-luminosity relation measured by Richer & McCall (1995) for a sample of dwarf galaxies, and by Tremonti et al. (2004) for SDSS star forming galaxies.

ples with high metallicity are galaxies with very high star formation rate (which coupled with the instantaneous recycling approximation, results in quite high metallicities of the inter-stellar medium).

4.3 The environment of LGRB host galaxies

The physical environment of LGRB host galaxies can provide important information on the origin of LGRBs. The analysis of GRB hosts environments is, however, quite difficult from the observational viewpoint, given the very low number of identified and well studied host galaxies. Only a few observational studies have attempted to address this question in the past few years. Gorosabel et al. (2003) used photometric redshift information in a field of $6' \times 6'$ containing the host galaxy of GRB 000210, and found no obvious galaxy concentration around the host. Bornancini et al. (2004) analysed the cross-correlation function between host galaxies and surrounding field galaxies using VLT and public HST data, and concluded that host galaxies do not reside in high density environments.

The semi-analytic catalogues used in our study provide the positions of the LGRB host galaxies, as well as of all other galaxies in the simulation box. We have used this information to study the auto-correlation function of host galaxies, and the cross-correlation function between hosts and all galaxies in the simulation (which we will call “normal” galaxies).

In order to compute the two-point correlation function, we adopt the Landy & Szalay (1993) estimator:

$$\xi(r) = \frac{DD(r) - 2DR(r)}{RR(r)} + 1 \quad (3)$$

where $DD(r)$ is the number of galaxy-galaxy pairs at distance r , $RR(r)$ is the number of random-random pairs, and $DR(r)$ is the number of random-galaxy pairs.

Fig. 10 shows the auto-correlation function for LGRB host galaxies in the HOST2 sample (dashed line) and for normal galaxies (solid line). The number of galaxies in the HOST3 sample are too low to compute a reliable correlation function. Results are shown for the WMAP3B model, but they are similar for the WMAP1 simulation. At low redshift, the auto-correlation function of host galaxies is lower than the corresponding function for normal galaxies. The difference between the two functions decreases with increasing redshift and the two functions almost perfectly overlap at $z > 4$. As explained in Sec. 4.1, this is due to the decrease of metallicity at high redshift which implies that an increasing fraction of the global galaxy population can host a LGRB event according to our selection (see Sec. 3).

The two point auto-correlation functions for the HOST2 sample and for normal galaxies at $z = 0$ is repeated in Fig. 11, together with the cross-correlation function between host and normal galaxies (solid line). The cross-correlation function lies in between the two auto-correlation functions, suggesting that the probability of finding another host near a GRB host is lower than the corresponding probability of finding a normal galaxy.

Our results are in qualitative agreement with those found by Bornancini et al. (2004) and suggest that LGRB host galaxies tend to populate regions with density lower than average. This is not entirely surprising if one considers that host galaxies are typically low-mass star forming galaxies which preferentially live in low density environments (Kauffmann et al. 2004).

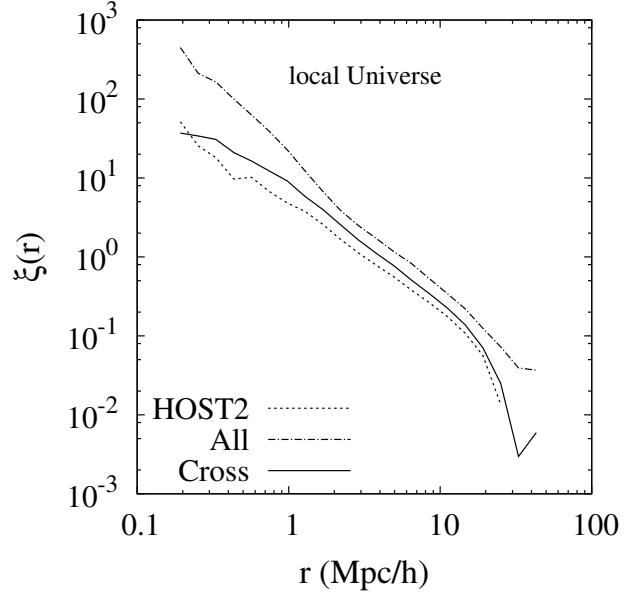


Figure 11. Two-point auto-correlation function for HOST2 galaxies (dashed line) and for normal galaxies (dot-dashed line) in the WMAP3B model. The solid line shows the cross-correlation function between host and normal galaxies.

4.4 Descendants of high- z LGRB host galaxies

From the theoretical point of view, it is interesting to ask which are the ‘descendants’ of high-redshift LGRB host galaxies. Do they preferentially end up in massive haloes? What are the typical morphology, colour, mass and metallicity of the descendants? While this is a very difficult (if not impossible) question to address observationally, it can be easily addressed with the available semi-analytic catalogues, which contain the full merger tree information for all galaxies in the simulation box.

In this section, we use this information to study the fate of LBRG host galaxies selected at $z \sim 4$ (hereafter *progenitors*) in the observed mass-metallicity and colour-magnitude planes, and the distribution of host halo virial mass of the descendant galaxies. For simplicity, we only show results for our HOST3 sample which contains a lower number of host galaxies than the HOST2 sample. Results are, however, similar for HOST2.

The top-left panel in Fig. 12 shows the mass-metallicity relation for our HOST3 sample at $z = 4.18$. The other panels show the location in the same plane of the descendant galaxies, down to $z = 0$. Galaxies are colour-coded as functions of their morphological types which are assigned by the ratio of the total bulge mass to the total stellar mass, B/T . Objects with $B/T > 0.5$ are classified as ‘ellipticals’ and are shown as red triangles, black diamonds represent ‘spirals’ ($B/T < 0.5$).

Fig. 12 shows that the LGRB host galaxies at redshift ~ 4 are low-mass and low-metallicity galaxies (as discussed in the previous sections), and that the great majority of them do not have a significant bulge component. At later time, galaxies grow in mass and their gas-phase metallicity increases. Fig 12 shows that the increase of the gas-phase metallicity is very rapid: a relatively large fraction of descendants at $z \sim 3$ already have solar metallicity [$12 + \log(\text{O}/\text{H}) \sim 8.7$, Allende Prieto et al. 2001] and most of the descendants at $z \sim 2$ have super-solar metallicity. This efficient enrichment of the interstellar medium is due to the fact that the semi-analytic model used in our study assumes a perfect mixing ef-

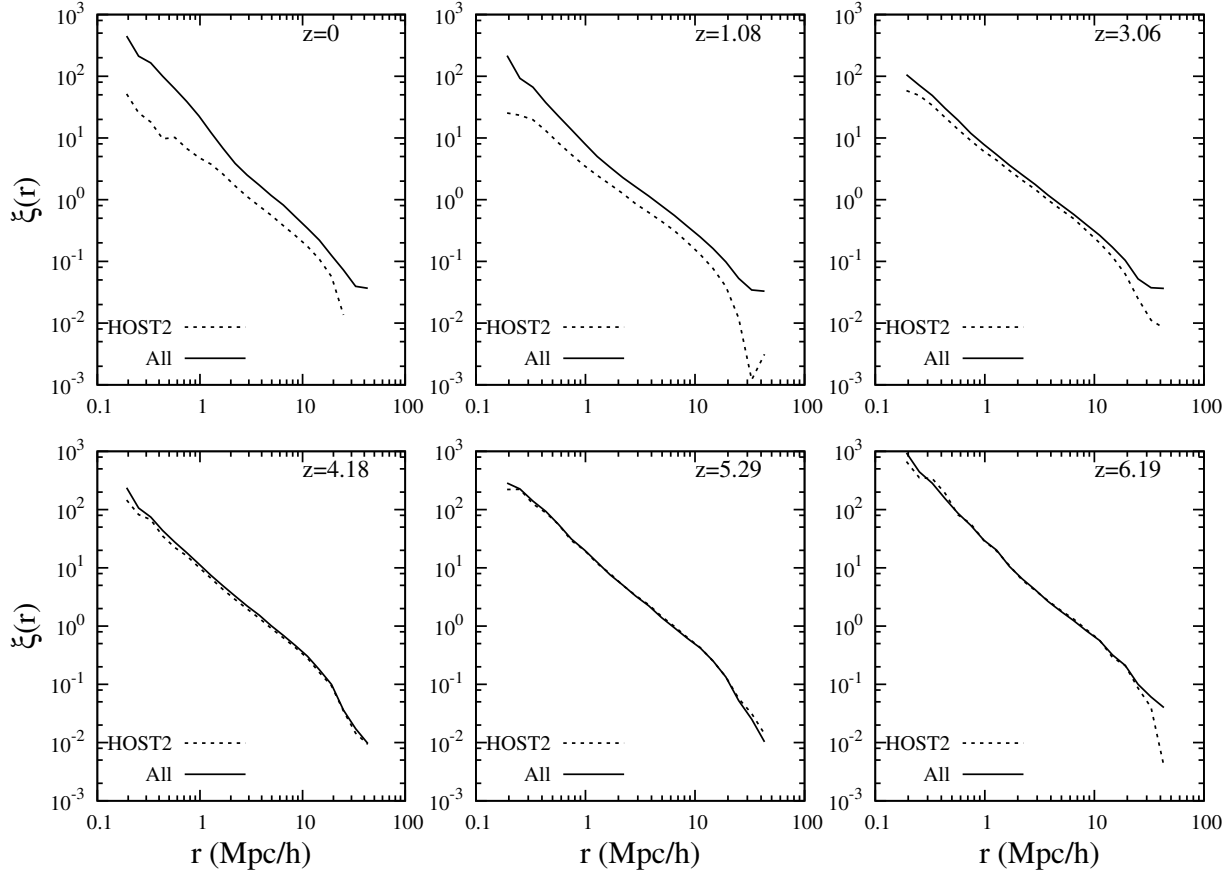


Figure 10. Two-point auto-correlation function for LGRB host galaxies from the HOST2 sample (dashed line) and for normal galaxies (solid line), at different redshifts, for WMAP3B cosmology.

efficiency of the metals formed by new stars (De Lucia et al. 2004). The stellar mass of the descendants evolves more slowly, with very few objects jumping to masses larger than $10^{11} M_{\odot}$, probably as a consequence of major mergers. At $z = 0$, all descendants of LGRBs at $z \sim 4$ have relatively high gas-phase metallicities and cover all the mass range between a few times 10^9 and $10^{12} M_{\odot}$. Interestingly, a large fraction of these (about 66 per cent) have a dominant bulge component.

Fig. 13 shows the location in the colour-magnitude diagram of LGRB host galaxies at $z = 4.18$ (top left panel) and of all their descendants at later time. LGRB hosts selected at $z \sim 4$ have very blue colours ($R-K < 1$) and relatively faint magnitudes. The descendants of these galaxies become progressively redder (they all have $R-K > 2$ at $z = 0$) and cover a wider range of magnitudes at low redshift. A few objects become very luminous and very red already at $z \sim 3$ (these are the same objects which appear very massive and metal rich at the same redshift in Fig. 12).

Finally, in Fig. 14 we show the parent halo mass of all descendant of LGRB host galaxies at $z \sim 4$ versus the halo mass of the host. The blue dashed line in each panel shows the one-to-one relation and is plotted to guide eyes. As expected, descendant galaxies reside in larger and larger haloes as time goes on. At $z \sim 2$, the majority of the descendant galaxies still reside in haloes of mass $\sim 10^{11} M_{\odot}$ but a few of them are in relatively massive haloes ($\sim 10^{14} M_{\odot}$) and are satellite galaxies of a very massive cluster at $z = 0$. In the local Universe, the descendants of high- z LGRB hosts reside in haloes of different mass but most of them still reside

in haloes with mass between 10^{12} and $10^{13} M_{\odot}$, in agreement with the results in Sec. 4.3.

5 DISCUSSION AND CONCLUSIONS

In this work, we have studied the physical and environmental properties of galaxies hosting Long Gamma-Ray Bursts (LGRBs) in the context of a hierarchical model of galaxy formation. In order to select host galaxies, we have adopted the collapsar model and used information available from a semi-analytic model of galaxy formation coupled to high-resolution cosmological simulations (Wang et al. 2008).

By imposing different metallicity constraints on the progenitor stars, we have constructed three host galaxies samples: HOST1 is built without any cut on the metallicity of progenitor stars of GRBs, while the HOST2 and HOST3 samples are constructed by selecting galaxies with progenitor stars of metallicity lower than $0.3Z_{\odot}$ and $0.1Z_{\odot}$ respectively.

A number of recent studies have adopted a similar but not identical approach to study the host galaxies of LGRBs. Nuza et al. (2007) developed a Monte Carlo code to identify hosts of LGRBs within a cosmological hydrodynamical simulations. Their analysis was also based on the collapsar model and limited to $z \leq 3$. The simulation used in Nuza et al. was relatively small ($10h^{-1}\text{Mpc}$) and therefore did not allow a detailed investigation of the environmental properties of LGRB hosts. As confirmed by our study, they pointed out that if LGRBs are generated by the death of mas-

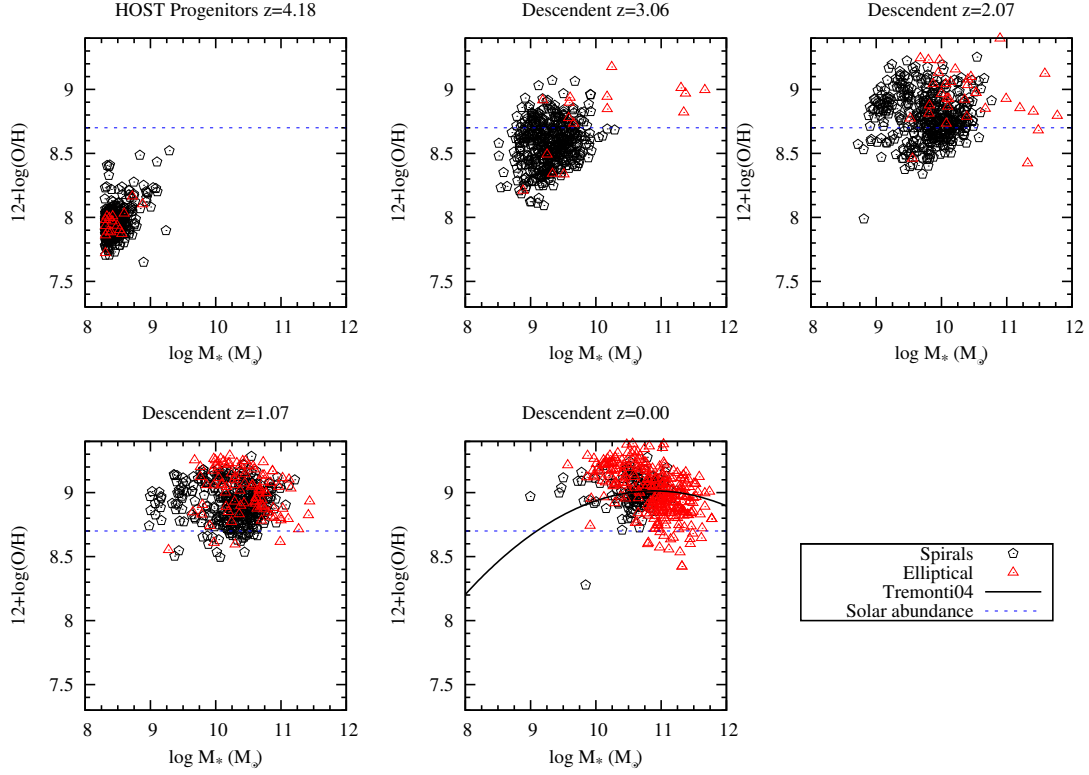


Figure 12. Mass-metallicity relation for HOST3 galaxies at redshift 4.18 (top left panel), and for their descendants at lower redshifts in the WMAP3B model. The colour coding indicates galaxies with different morphologies (red triangles for ellipticals and black diamonds for spirals). The solid black line in the bottom right panel shows the best fit relation found by Tremonti et al. (2004). The horizontal dashed line corresponds to the adopted solar abundance.

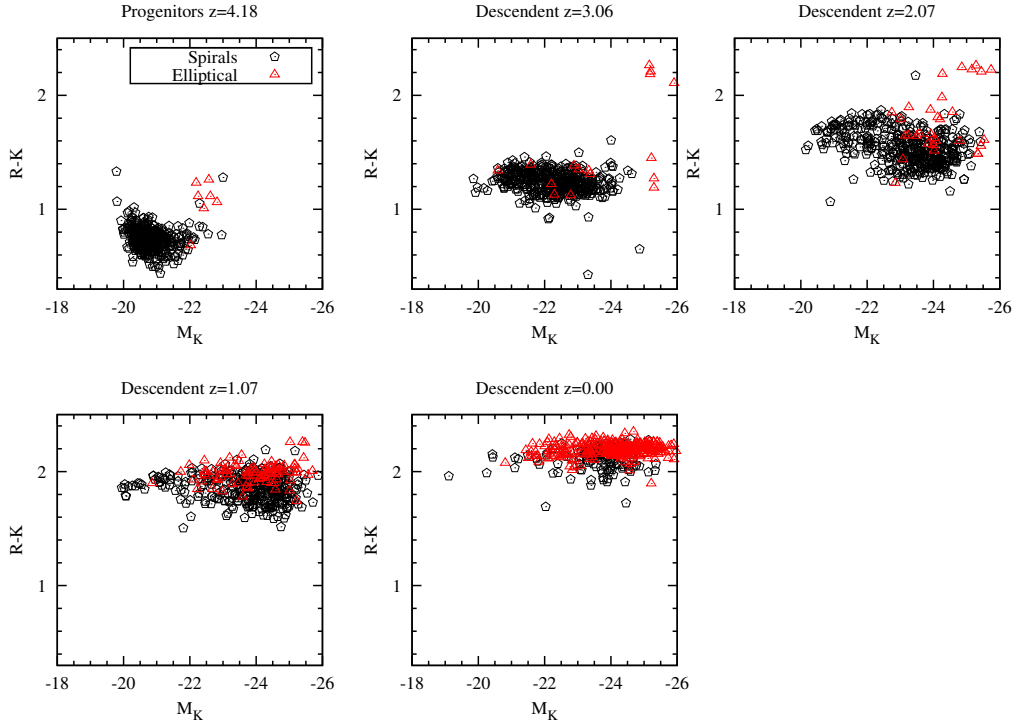


Figure 13. $R-K$ colour as a function of the K-band magnitude for HOST3 galaxies at $z \sim 4$ (top-left panel), and for their descendants at lower redshifts in the WMAP3B model. Red triangles are for elliptical galaxies while black diamonds are for spirals.

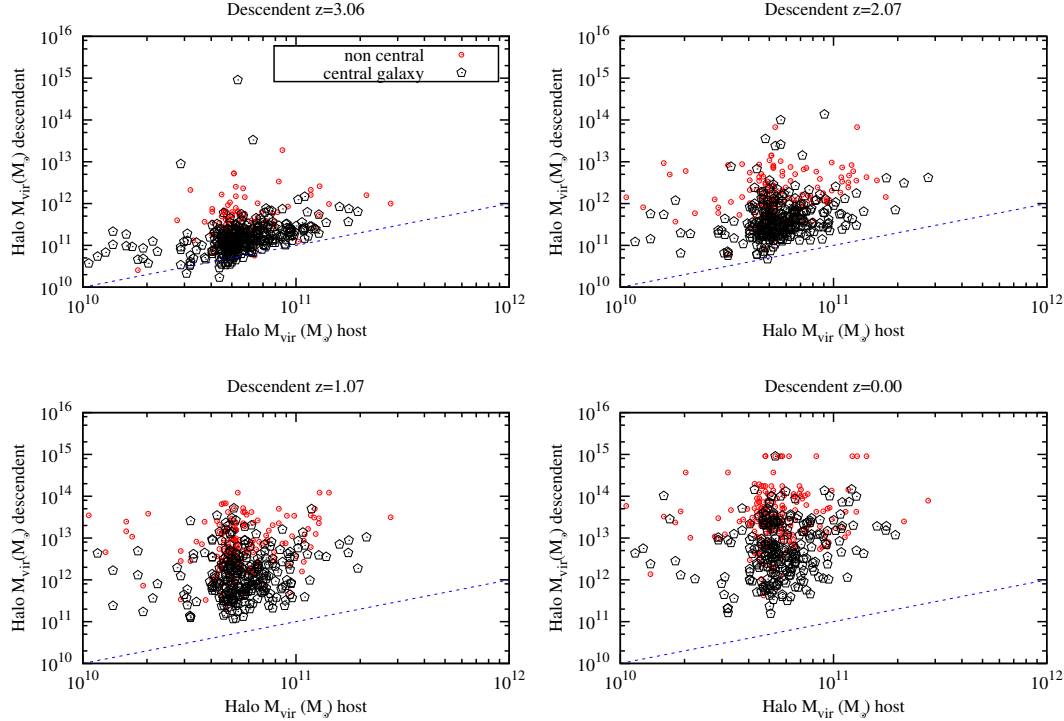


Figure 14. Parent halo mass of all descendants of HOST3 galaxies selected at $z = 4.18$, as a function of the halo mass of the host galaxies in the WMAP3B case. Red symbols are used for satellite galaxies and black symbols for central galaxies.

sive young stars of metallicity lower than a certain value, they do not provide a good tracer of the cosmic star formation history (see Sec. 4.1 and later).

Lapi et al. (2008) used the cosmological star formation rate below a critical metallicity to estimate the event rate of LGRBs. To this purpose, they employed the galaxy formation model presented in Granato et al. (2004). Lapi et al. find that their predicted number counts of LGRBs agrees well with the bright *SWIFT* data, without the need for an intrinsic luminosity evolution. They find that host galaxies are dominated by young stellar populations, are gas rich and metal-poor. The model adopted in Lapi et al. (2008) does not follow galactic disks nor does it consider mergers between galaxies or between haloes. In addition, the model does not provide spatial information of model galaxies.

In another recent study, Courty et al. (2007) used N-body/Eulerian hydrodynamic simulations, and identified GRB host galaxies with those having SFR and SFR-to-luminosity similar to those of 10 observed GRB hosts in the redshift range $0.43 < z < 2.03$. They found that the host galaxies have low stellar masses and low mass-to-light ratios, are young and bluer than typical galaxies at the same cosmic epochs. Their identification of simulated galaxies with observed hosts is limited by uncertainties on the observational estimates of the SFR and luminosity of host galaxies. In addition, their simulated volume is relatively small ($32 h^{-1}$ Mpc) and the analysis is limited to relatively low redshifts.

Compared to previous works, our study uses a much larger simulated volume (a box of $125 h^{-1}$ Mpc on a side - see Sec. 2) that allows us to study the environmental properties of model host galaxies. In addition, the use of two different cosmological models allows us to analyse the dependence of results on cosmology. The semi-analytic model employed in our work has been studied in a number of previous papers, and it has been shown to successfully

reproduce a number of observational results for the global galaxy population in the local Universe and at higher redshift (see Sec. 2).

In agreement with previous work, and as expected due to the global increase of the ISM metallicity with decreasing redshift, we find that when assuming a metallicity threshold for progenitor stars of LGRBs, they do not represent a perfect tracer of the cosmic star formation history. The bias is stronger as the metallicity threshold assumed is lowered. At higher redshift, the cold-phase metallicity of model galaxies is lower, and galaxies form stars at higher rates. As a consequence, there is a higher rate of LGRBs per galaxy and the host galaxy population includes a larger fraction of the global galaxy population, with the two populations sharing very similar physical properties.

At lower redshift, the host galaxy population is dominated by galaxies with low-masses, relatively young ages, blue colours, and luminosity below L_* , in qualitative agreement with observational measurements. We note, however, that while ~ 90 per cent of the galaxies in our simulations have stellar masses lower than $\sim 10^{10} M_{\odot}$, only ~ 0.3 per cent of them are in the HOST3 sample and ~ 13 per cent in the HOST2 sample.

The metal content and metallicity evolution of host galaxies also appear to be in agreement with observational estimates. Since in the model adopted in this study stars form with the metallicity of the cold-phase component at the time of the star formation, host galaxies have average metallicity lower or close to the metallicity threshold adopted. Metallicity studies of LGRB host galaxies could therefore provide important constraints on the adopted collapsar model. It is important to note, however, that inhomogeneous mixing of metals (which is not considered in the model adopted here) could significantly complicate this picture. The metal content of host galaxies does not significantly evolve with redshift, while the overall galaxy population exhibit some weak evolution.

Taking advantage of the spatial information provided by the semi-analytic model used in our work, we study the clustering properties of model host galaxies and compare them to the corresponding properties of the global galaxy population. Since a larger fraction of the whole galaxy population can host LGRBs at high redshift, the clustering properties of host galaxies do not differ significantly from the clustering properties of ‘normal’ galaxies. At lower redshift, the host galaxies are significantly less clustered than normal galaxies, as expected due to their physical properties. Interestingly, we find that the cross-correlation function between host and normal galaxies lies in between the the auto-correlation functions of host galaxies and normal galaxies, suggesting that the probability of finding another host galaxy nearby a GRB host is lower than the corresponding probability of finding a normal galaxy. This implies that LGRBs reside in regions with density lower than average. When larger samples of LGRB host galaxies will become available, it will be possible to test our clustering predictions.

Using the available semi-analytic catalogues, which contain the full merger tree information for all galaxies in the simulation box, we find that LGRB host galaxies at redshift ~ 4 (which have low stellar mass, low metallicity and no significant bulge component) evolve into relatively massive, red galaxies at redshift zero. While the descendants of high- z LGRBs reside in haloes of different mass in the local Universe, most of them still sit in haloes with mass between 10^{12} and $10^{13} M_{\odot}$.

ACKNOWLEDGEMENTS

We are indebted to Dr. Jie Wang for making available their simulated galaxy catalogues and simulation outputs. We thank Sandra Savaglio for useful discussions. SM would like to acknowledge the Humboldt Foundation for travel support. We also acknowledge an anonymous referee for a constructive report that improved the paper.

REFERENCES

- Allende Prieto C., Lambert D. L., Asplund M., 2001, *ApJ*, 556, L63
- Bornancini C. G., Martínez H. J., Lambas D. G., Le Floch E., Mirabel I. F., Minniti D., 2004, *ApJ*, 614, 84
- Bromm V., Loeb A., 2002, *ApJ*, 575, 111
- Brown W. R., Kewley L. J., Geller M. J., 2008, *AJ*, 135, 92
- Campisi M. A., Li L.-X., 2008, *ArXiv e-prints*, accepted by *MNRAS*, 809
- Castro Cerón J. M., Michałowski M. J., Hjorth J., Malesani D., Gorosabel J., Watson D., Fynbo J. P. U., 2008, *ArXiv e-prints*, 803
- Cen R., Fang T., 2007, *ArXiv:0710.4370*
- Conselice C. J., Vreeswijk P. M., Fruchter A. S., Levan A., Kouveliotou C., Fynbo J. P. U., Gorosabel J., Tanvir N. R., Thorsett S. E., 2005, *ApJ*, 633, 29
- Courty S., Björnsson G., Gudmundsson E. H., 2007, *MNRAS*, 376, 1375
- Croton D. J., Springel V., White S. D. M., De Lucia G., Frenk C. S., Gao L., Jenkins A., Kauffmann G., Navarro J. F., Yoshida N., 2006, *MNRAS*, 365, 11
- Dai Z. G., Liang E. W., Xu D., 2004, *ApJ*, 612, L101
- De Lucia G., Blaizot J., 2007, *MNRAS*, 375, 2
- De Lucia G., Kauffmann G., White S. D. M., 2004, *MNRAS*, 349, 1101
- De Lucia G., Springel V., White S. D. M., Croton D., Kauffmann G., 2006, *MNRAS*, 366, 499
- Fan Y.-Z., Piran T., 2008, *Frontiers of Physics in China*, 3, 306
- Fruchter A. S., Levan A. J., Strolger e. a., 2006, *Nature*, 441, 463
- Fryer C. L., Woosley S. E., Hartmann D. H., 1999, *ApJ*, 526, 152
- Fynbo J. P. U., Prochaska J. X., Sommer-Larsen J., Dessauges-Zavadsky M., Møller P., 2008, *ApJ*, 683, 321
- Fynbo J. P. U., Watson D., Thöne C. C., Sollerman J., Bloom J. S., Davis T. M., Hjorth J., Jakobsson P., Jørgensen U. G., Graham J. F., Fruchter A. S., Bersier D., Kewley L., Cassan A., Castro Cerón J. M., Foley e. a., 2006, *Nature*, 444, 1047
- Galama T. J., Vreeswijk P. M., van Paradijs J., Kouveliotou C., Augusteijn T., Bönnhardt H., Brewer J. P., Doublier V., Gonzalez J.-F., Leibundgut B., Lidman C., Hainaut O. R., Patat F., Heise J., in’t Zand J., Hurley e. a., 1998, *Nature*, 395, 670
- Ghirlanda G., Ghisellini G., Lazzati D., 2004, *ApJ*, 616, 331
- Gorosabel J., Christensen L., Hjorth J., Fynbo J. U., Pedersen H., Jensen B. L., Andersen M. I., Lund N., et al. 2003, *A&A*, 400, 127
- Huang Y. F., Gou L. J., Dai Z. G., Lu T., 2000, *ApJ*, 543, 90
- Kauffmann G., White S. D. M., Heckman T. M., Ménard B., Brinchmann J., Charlot S., Tremonti C., Brinkmann J., 2004, *MNRAS*, 353, 713
- Kistler M. D., Yüksel H., Beacom J. F., Stanek K. Z., 2008, *ApJ*, 673, L119
- Kitzbichler M. G., White S. D. M., 2007, *MNRAS*, 376, 2
- Kouveliotou C., Meegan C. A., Fishman G. J., Bhat N. P., Briggs M. S., Koshut T. M., Paciesas W. S., Pendleton G. N., 1993, *ApJ*, 413, L101
- Landy S. D., Szalay A. S., 1993, *ApJ*, 412, 64
- Langer N., Norman C. A., 2006, *ApJ*, 638, L63
- Lapi A., Kawakatu N., Bosnjak Z., Celotti A., Bressan A., Granato G. L., Danese L., 2008, *MNRAS*, 386, 608
- Le Floch E., Duc P.-A., Mirabel I. F., Sanders D. B., Bosch G., Diaz R. J., Donzelli C. J., Rodrigues I., Courvoisier T. J.-L., Greiner J., Mereghetti S., Melnick J., Maza J., Minniti D., 2003, *A&A*, 400, 499
- Li L.-X., 2006, *MNRAS*, 372, 1357
- Li L.-X., 2007a, *MNRAS*, 374, L20
- Li L.-X., 2007b, *MNRAS*, 379, L55
- Li L.-X., 2008a, *Acta Astronomica*, 58, 103
- Li L.-X., 2008b, *MNRAS*, 388, 1487
- Li L.-X., Paczyński B., 1998, *ApJ*, 507, L59
- Mao S., Mo H. J., 1998, *A&A*, 339, L1
- Nuza S. E., Tissera P. B., Pellizza L. J., Lambas D. G., Scannapieco C., de Rossi M. E., 2007, *MNRAS*, 375, 665
- O’Shaughnessy R., Belczynski K., Kalogera V., 2008, *ApJ*, 675, 566
- Porciani C., Madau P., 2001, *ApJ*, 548, 522
- Price P. A., Cowie L. L., Minezaki T., Schmidt B. P., Songaila A., Yoshii Y., 2006, *ApJ*, 645, 851
- Price P. A., Songaila A., Cowie L. L., Bell Burnell J., Berger E., Cucchiara A., Fox D. B., Hook I., Kulkarni S. R., Penprase B., Roth K. C., Schmidt B., 2007, *ApJ*, 663, L57
- Prochaska J. X., Bloom J. S., Chen H.-W., Hurley K. C., Melbourne J., Dressler A., Graham J. R., Osip D. J., Vacca W. D., 2004, *ApJ*, 611, 200
- Prochaska J. X., Chen H.-W., Dessauges-Zavadsky M., Bloom J. S., 2007, *ApJ*, 666, 267
- Richer M. G., McCall M. L., 1995, *ApJ*, 445, 642

- Salvaterra, R., et al. 2009, arXiv:0906.1578
- Savaglio S., 2006, *New Journal of Physics*, 8, 195
- Savaglio S., Fall S. M., Fiore F., 2003, *ApJ*, 585, 638
- Savaglio S., Glazebrook K., Le Borgne D., 2008, *ArXiv e-prints*, 803
- Spergel D. N., Verde L., Peiris H. V., Komatsu E., Nolte M. R., Bennett C. L., Halpern M., Hinshaw G., Jarosik N., Kogut A., Limon M., Meyer S. S., Page L., Tucker G. S., Weiland J. L., Wollack E., Wright E. L., 2003, *ApJS*, 148, 175
- Springel V., White S. D. M., Jenkins A., Frenk C. S., Yoshida N., Gao L., Navarro J., Thacker R., Croton D., Helly J., Peacock J. A., Cole S., Thomas P., Couchman H., Evrard A., Colberg J., Pearce F., 2005, *Nature*, 435, 629
- Stanek K. Z., Gnedin O. Y., Beacom J. F., Gould A. P., Johnson J. A., Kollmeier J. A., Modjaz M., Pinsonneault M. H., Pogge R., Weinberg D. H., 2006, *Acta Astronomica*, 56, 333
- Tanvir, N. R., et al. 2009, arXiv:0906.1577
- Totani T., 1997, *ApJ*, 486, L71
- Totani T., Kawai N., Kosugi G., Aoki K., Yamada T., Iye M., Ohta K., Hattori T., 2006, *Astronomical Society of Japan*, 58, 485
- Tremonti C. A., Heckman T. M., Kauffmann G., Brinchmann J., Charlot S., White S. D. M., Seibert M., Peng E. W., Schlegel D. J., Uomoto A., Fukugita M., Brinkmann J., 2004, *ApJ*, 613, 898
- Wainwright C., Berger E., Penprase B. E., 2007, *ApJ*, 657, 367
- Wang J., De Lucia G., Kitzbichler M. G., White S. D. M., 2008, *MNRAS*, 384, 1301
- Wijers R. A. M. J., Bloom J. S., Bagla J. S., Natarajan P., 1998, *MNRAS*, 294, L13
- Wolf C., Podsiadlowski P., 2007, *MNRAS*, 375, 1049
- Woosley S. E., Heger A., 2006, *ApJ*, 637, 914
- Yoon S.-C., Langer N., Cantiello M., Woosley S. E., Glatzmaier G. A., 2008, in *IAU Symposium Vol. 250 of IAU Symposium, Evolution of Progenitor Stars of Type Ibc Supernovae and Long Gamma-Ray Bursts*. pp 231–236
- Yoon S.-C., Langer N., Norman C., 2006, *A&A*, 460, 199
- Zhang B., 2007, *Chinese Journal of Astronomy and Astrophysics*, 7, 1
- Zhang B., Mészáros P., 2004, *International Journal of Modern Physics A*, 19, 2385